

# Theoretical Evaluation of Resonator Fiber Optic Gyroscope Composed of a Polarization-Maintaining and Single Mode fiber with Digital Phase Modulation Technique

Prasada Rao Bobbili<sup>1</sup>, Jagannath Nayak<sup>2</sup>, Prerana dabral pinnoji<sup>3</sup>  
and D.V. Rama Koti reddy<sup>4</sup>

<sup>1,4</sup> Dept. of Instrument Technology, AUCE, Andhra University, Visakhapatnam, India.

<sup>2,3</sup> Electro-optical Instruments Research Academy (ELORA), Hyderabad, India.

<sup>1</sup>bvvprasadarao@gmail.com, <sup>2</sup>nayak\_jagannath@rediffmail.com, <sup>3</sup>preranadabral@gmail.com, <sup>4</sup>rkreddy\_67@yahoo.co.in

[www.ijcseonline.org](http://www.ijcseonline.org)

Received: Mar/30/2015

Revised: Apr/12/2015

Accepted: Apr/18/2015

Published: Apr/30/ 2015

**Abstract:** Resonator fiber optic gyroscope (RFOG) based on the Sagnac effect has the potential to achieve the inertial navigation system condition with a short sensing coil. RFOG based on fiber coupled semiconductor DFB-LD with an FPGA-based digital processor is set up. We evaluate the frequency drift due to the various non-reciprocal noise sources –shot-noise; backscattering, Shupe, Kerr effect and Faraday noises are calculated theoretically with single mode fiber (corning SMF-28) as sensor coil and compared with PM fiber (HB 1500G) as sensing coil with similar parameters. Bias of the gyro which is caused by the noise source is also analysed.

**Keywords:** Bias Drift, Digitalization, Noise sources, Optical fiber gyroscope, Optical passive ring-resonator gyro scope, PM fiber, SM Fiber.

## I. INTRODUCTION

Optical fiber gyros based on the Sagnac effect have been extensively studied for rotation measurement in applications such as navigation, oil platform stabilization, and well logging. Compared to an interferometric fiber optic gyro (IFOG), resonator fiber optic gyroscope (RFOG) uses a high finesse fiber ring resonator and a highly coherent laser source which has the potential to achieve similar shot-noise of limited performance with a shorter fiber length [1,2]. However, the performance of an OPRG made of conventional single mode fiber (SMF) In this paper, we analyse numerically the measurement errors due to Kerr, Faraday and Shupe effects, and Rayleigh backscattering in an RFOG a PM fiber sensing coil, and compare the same with a conventional SMF sensing coil.

## II. PRINCIPLES AND EXPERIMENTS

### 2.1. RFOG configuration

Figure .1. Depicts the experimental setup for the RFOG with sinusoidal phase modulation controlled by the proposed FPGA-based digital processor. A 1550 nm fiber-coupled semiconductor DFB-LD, whose line width is less than 10 KHz, is used as the light source. Two sinusoidal modulation signal generators, two synchronous demodulators, as well as a proportional integrator are realized in this FPGA itself. Light wave from the DFB-LD is equally divided by a coupler C1 and injected into the Resonator fiber optic gyro (RFOG) in

is limited by a number of deleterious effects that arise from the undesirable properties of the sensing fiber, namely: Kerr [3], Faraday [4], and Shupe [5] effects and Rayleigh backscattering [6]. Though counter measures were proposed to minimize these effects, they are not perfect and tend to increase the complexity and cost of the gyros [2, 7, and 8]. So far the performance of RFOGs is inferior to that of IFOGs.

Recent advance in polarization maintaining (PM) fibers offers a radically new means of minimizing these unwanted effects, which would reduce the complexity, size, and cost of RFOGs.

Clockwise (CW) and Counter Clockwise (CCW) light waves. PM1 and PM2 are driven by sinusoidal waveforms with modulation frequencies  $f_1$  and  $f_2$  respectively. The amplitudes of the two sinusoidal voltage waves  $V_1$  and  $V_2$  are carefully optimized to reduce the backscattering induced noise [9]. The CW and the CCW light waves from the optical fiber ring resonator (OFRR) are detected by the In GaAs PIN photo detectors PD1 and PD2, respectively. The output of PD1 is fed back through the digital lock-in amplifier to adjust the central frequency of the DFB-LD to be locked at the resonance frequency of the CCW light wave in the OFRR. The demodulated signal of CW light wave from LIA1 is used as the open-loop readout of the rotation rate.

The polarization maintaining OFRR with twin 90° polarization-axis rotated splices is adopted to reduce the polarization induced noise [10]. It is wound around a 12-cm diameter spool. The total length of the OFRR is 12m.

As a result, the free spectral range (FSR) of the OFRR becomes 17.24 MHz

Based on the system shown in fig.1, a saw tooth-wave signal from a signal generator tunes the central frequency of the DFB-LD linearly with respect to time, and no lock-in process is contained. Fig.2 shows the measured resonant curve of the OFRR observed in PD1. The measured finesse is approximately 50. Only a single linear Eigen State of Polarization (ESOP) is excited and the other unwanted ESOP is almost suppressed through controlling the two splicing positions in the OFRR as shown in fig.2.

If the OPRG is operated in an open-loop configuration and  $f_0$  and  $f_r$  are central frequency of the laser and resonant frequency of the resonator, the frequency difference  $\Delta f = f_0 - f_r$  is related to the rotation rate by,

$$\Delta f = \frac{4A}{\lambda P} \Omega \tag{1}$$

Where  $\lambda$  is the wavelength of the source in vacuum, P is the optical perimeter of the resonator, and A is the area enclosed by the resonator.

Instead of locking at the centre of the respective resonances, the CW and CCW light frequencies can also be locked to a higher slope point on either side of the resonance, yet the relation between the  $\Delta f$  and  $\Omega$  is given by Eq.(1).

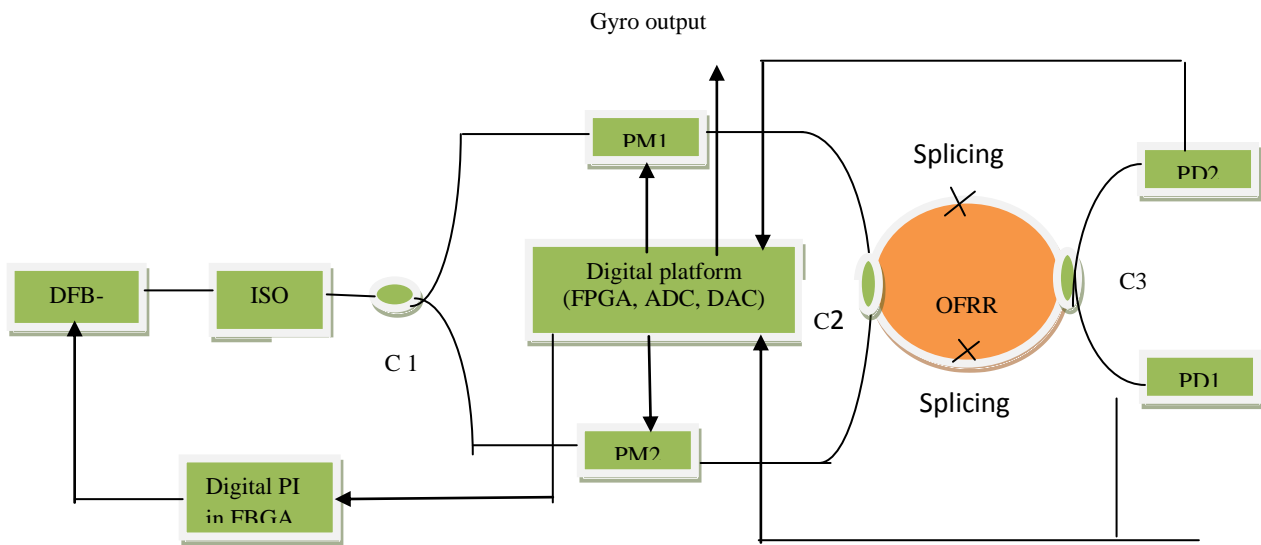


Fig.1. Experimental set up of the RFOG with the proposed FBGA Based digital processor

### 2.2 The gyro signal

When stationary, the output voltage at detector D1 may be expressed as [2]

$$V_{out} = (1 - \gamma) \left[ 1 - \frac{(1 - K_r)^2}{(1 + K_r)^2 - 4K_r \sin^2\left(\frac{\beta L}{2} - \frac{\pi}{4}\right)} \right] \tag{2}$$

Where  $\gamma$ ,  $K_r$  and  $\beta L$  are fractional coupling intensity loss, resonant coupling coefficient and resonance phase angle.

The shape and resonance depth of the output are related to source spectrum, the resonator parameters (i.e., coupling ratio and loss of coupler C2, length and

attenuation of the sensing fiber coil). The normalized transmission of the resonator as a function of wavelength is illustrated in fig.2. The Lorentzian resonance curve is characterized by the FWHM line width,  $\Gamma$ , with maximum and the minimum transmission  $T_{max}=0.5747$  and  $T_{min}=0.0007$ , which are also indicated in fig.2 and will be used later to calculate the measurement uncertainties due to shot and backscatter noise. When gyro rotates, the CW and CCW resonances split and difference in the resonance frequencies is given by Eq. (1).

However, the measurement of  $f_r$  and hence  $\Delta f$  are corrupted by noises and errors due to various deleterious effects as mentioned in section .1. The uncertainty  $\delta f$  in measuring  $\Delta f = f_0 - f_r$  and the resulting uncertainty  $\delta \Omega$  in measuring  $\Omega$  are related by v

$$\delta \Omega = \delta f * \frac{\lambda P}{4A} \tag{3}$$

$$SNR = \frac{\eta t_o E_o (T_{max} - T_{min})}{\sqrt{2h f_o} \sqrt{T_{max}}} \quad (5)$$

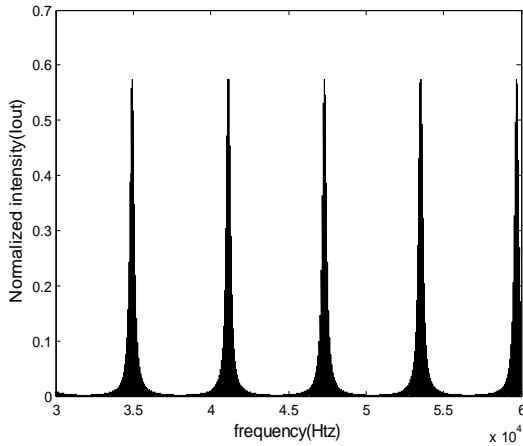


Fig.2. Normalized transmission as a function of resonator phase angle.

The main source of errors/noises are the backscattered waves [6, 8] that mix coherently with the signal waves and generate unwanted intensity fluctuation, which is added to the resonator output and effect the accuracy in locking the central frequency to the resonant frequency of the coil; and Kerr [3, 7], Faraday [4], and Shupe [5] effects that induce non-reciprocal phase changes are indistinguishable from the rotation-induced phase change. Total bias drift due to the effecting noises is,

$$\delta\Omega = \delta\Omega_s + \delta\Omega_B + \delta\Omega_T + \delta\Omega_K + \delta\Omega_F \quad (a)$$

In this paper, we evaluate bias drift of gyro numerically due to the impact of these deleterious effects on the performance of an OPRG with a PM fiber (HB 1500G) sensing coil and compare it with 3232, an OPRG with a conventional fiber (corning SMF-28) sensing coil with similar system parameters. The common parameters used in the calculation are: coupling ratio of C1: 50%, coupling ratio of C2, C3: 5% and 95%, input power: 50μW, wave length of the laser: 1550nm, radius of the sensing coil: 5cm, effective index  $n_e$  of the fundamental mode: 1.4571 for PM fiber and 1.4682 for conventional SMF, fiber attenuation: 2dB/km for PM fiber and 0.05dB/km for conventional SMF.

### III. NUMERICAL ANALYSIS

#### 3.1 Shot-noise limit

Shot noise at the output of the photo-detector is directly added to the signal output voltage that is proportional to  $V_{out}$  as given in eq. (2). This results in measuring uncertainty in  $f_o$ , and hence  $\delta f$  and  $\delta\Omega$ . When operating around the centre of the resonance ( $\beta L = 2m\pi + \pi$ ), the shot-noise limited measurement error  $\delta\Omega_s$  may be expressed as [5, 11]

$$\delta\Omega_s \approx \frac{\lambda P \sqrt{2I}}{4A SNR} \quad (4)$$

Where  $\eta$  is the photo detector quantum efficiency,  $t_o$  the integration time,  $E_o$  is the laser intensity inputting to coupler C2, and  $h$  is Plank's constant.

PM fiber is different from conventional SMF in terms of attenuation and Eigen state of polarization and other factors such as coupler coupling ratio and excess loss affect the resonance curve and hence  $\delta\Omega_s$ . With Eqns. (4) and (5),  $\eta = 0.8$ ,  $t_o = 1s$ , the bias drift due to shot noise for SM and PM fiber as sensing coil are  $\delta\Omega_s = 1.7e^{-70}/sec$ ,  $\delta\Omega_s = 1.66e^{-60}/sec$ .

#### 3.2 Backscattering noise

An OPRG needs a coherent light source to achieve high performance. However, the long coherent length increases the backscatter noise due to the coherent mixing of CW (CCW) signal beam and the backscattered/reflected waves from the CCW (CW) signal. When backscatter noise is considered, the signal at photo-detector D1 may be expressed as [6]

$$I = I_1 + \sigma + \langle I_3 \rangle \quad (6)$$

Where  $\sigma$  is the interference intensity which is due to coherent mixing between the signal and the backscattered waves and has a similar resonance characteristic as the signal beam. The magnitude of  $\sigma$  may be estimated by [6]

$$\sigma = 2T I_o \sqrt{\alpha_B S_B L (Cr^2 + Ci^2)} \quad (7)$$

Where  $T$ ,  $Cr$ , and  $Ci$  are related to gyro parameters and are defined in reference [4],  $\alpha_B$  is the backscattering coefficient and  $S_B = ((NA/n)^2)/2$  is the recapture factor of the fiber.  $\langle I_3 \rangle$  represents the backscattered beam intensity, and is given by Eq. (18) in reference [6]. The interference intensity  $\sigma$  and Backscattering beam intensity are fluctuating with environment and they introduce measurement errors. The signal to noise ratio (SNR) due to coherent backscatter may be expressed as Eq. (8).

$$SNR_B = \frac{I_o (T_{max} - T_{min})}{\sigma} \quad (8)$$

Substituting Eq. (8) into Eq. (4), and with the following parameters  $\alpha_B = 3.3617e^{-4}$ ,  $NA = 0.17$  for PMF;  $\alpha_B = 3.4131e^{-4}$ ,  $NA = 0.14$  for SMF. Theoretically, the bias drift due to backscattering noise for SM and PM fiber as sensing coil are  $\delta\Omega_B = 0.54 /sec$ ,  $\delta\Omega_B = 6.4 /sec$ .

#### 3.3 Shupe effect

The phase  $\Phi$  accumulated by the fundamental mode as it propagates through a fiber of length  $L$  depends on temperature through thermal expansion of the fiber, the

thermal-optic effect and the variation of the transverse dimension.

In a fiber ring resonator, thermally induced non-reciprocity can occur if there is a time-dependent temperature gradient along the fiber. Non-reciprocity arises when the corresponding wave fronts in the two counter-rotating beams transverse the same region of the fiber at different times. If the fiber propagation constant varies at different rates along the fiber, the corresponding wave fronts in the two counter-rotating beams transverse a slightly different effective path. This creates a non-reciprocal phase shift that is indistinguishable from the phase shift caused by rotation [5]:

$$\delta\Omega_T = \frac{n^2 SL \Delta T}{12\alpha} \quad (9)$$

$$S = \left( \alpha + \frac{1}{n} \frac{dn}{dT} \right) = S_L + S_n \quad (10)$$

S is the Shupe constant and includes two terms: the length term  $S_L$ , and the index term  $S_n$ .  $\alpha$  is the coefficient of thermal expansion of the fiber, L is the length of the sensing coil,  $\Delta T$  is the temperature difference between the inner and outer layers, and a, the radius of the fiber coil. Equation. (9) shows that the thermal sensitivity of the OPRG is proportional to the Shupe constant S, and the mode index (n). And we observed theoretically bias drift due to Shupe effect as SM fiber as a sensor coil  $7.8e^{-60}/\text{sec}$  and PM as a  $2.4e^{-50}/\text{sec}$ .

### 3.4 Kerr effect

The drift  $\delta\Omega_k$  due to the Kerr effect may be expressed as [3]

$$\delta\Omega_k = \frac{c\lambda\delta}{4\pi L\alpha} \left[ \Delta u + \frac{\sqrt{2} R_f}{1-R_f} \Delta\Phi \right] \quad (11)$$

$$\delta = \frac{\eta n_2}{A^* c (1-t_f^2)} \frac{2\omega}{\alpha l} \rho e^{-\alpha c} I_0 \quad (12)$$

Where  $\Delta u = u_{cw} - u_{ccw}$ , and  $u_{cw}$  and  $u_{ccw}$  are the beam-splitting coefficients of two counter-propagating beams. For ideal equal beam splitting,  $u_{cw} = u_{ccw}$ .  $\Delta\Phi$  is the difference in the phase modulation amplitudes that are used in the input ends of the resonator for minimizing the coherent backscatter/reflection noise. H,  $A^*$ , and  $n_2$  are the impedance of the fiber, the mode field area, and the Kerr coefficient, respectively.  $T_f$  is transmission

through the fiber coil. The Kerr coefficient may be expressed as [10]:

$$n_2, PBF = \chi n_2, \text{silica} + (1 - \chi) n_2, \text{air} \quad (13)$$

Using Eq. (11) and the following parameters [3]: for conventional SMF (corning SMF-28),  $\eta=259.81$ , mode field diameter= $10.6\mu\text{m}$ ; for PM fiber (HB 1500G),  $\eta=100$ . Mode field diameter= $7.9\mu\text{m}$  and  $\chi=0.002$ . We numerically calculated the rotation rate error induced by optical Kerr effect in the OPRG with a PMF coil, and compare it with the conventional SMF OPRG. The drift due to Kerr effect -SM fiber as sensing coil  $6.7e^{-15} \text{ }^\circ/\text{sec}$  and PM fiber as a sensing coil  $2.17e^{-120}/\text{sec}$ .

### 3.5 Faraday Effect

The drift of an IFOG due to Faraday Effect has been analysed by Hotate and Tabe [4]. For an OPRG with a N-turn coil in a magnetic field  $H_o$ , the variation of the phase difference between the CW and CCW beams in one round trip may be obtained by following a similar analysis and given by

$$|\delta\psi| = \frac{8\alpha\zeta_0}{\Delta\beta} |\Phi| \quad (13)$$

$$\Phi = \int_0^{2N\pi} \phi(\theta) \exp(-j\theta) (d\theta) \quad (14)$$

Where  $\zeta_0 = V H_o$  representing the maximum Faraday rotation per unit length under  $H_o$ , V is the effective Faraday constant of the fiber. A is the radius of the fiber coil, and  $\Delta\beta$  and  $\phi$  are respectively the birefringence and the twist per unit length. By using Eq. (3) and  $\delta\psi=2\pi.\delta f.\tau_0$ , the gyro drift in terms of rotation rate may be expressed as

$$\delta\Omega_F = \frac{\lambda P}{4A} \delta f = \frac{\lambda P}{4A} \frac{\delta\psi}{2\pi\tau_0} = \frac{2\lambda c}{\pi L} \frac{V H_o}{\Delta\beta} \sqrt{2N\pi W} \quad (15)$$

From Eq. (15), several observations may be made. Firstly  $\delta\Omega_F$  is proportional to  $|\Phi|$ , the twist of the fiber in the coil. Under ideal condition no twist exists, the magnetic field would have no effect on the gyro drift.

Secondly,  $\delta\Omega_F$  is inversely proportional to the fiber birefringence and hence can be reduced by using PM fiber with a high birefringence. We observed theoretically bias drift  $4.47e^{-80}/\text{sec}$ , SM fiber as sensing coil and  $4.5e^{-7}/\text{sec}$ , PM fiber as a sensing coil.

## IV.RESULTS AND DISCUSSION

S.No.	Noise Source	Drift due to SM Fiber as a sensor coil. ( $^\circ/\text{sec}$ ).	Drift due to PM Fiber as a sensor coil. ( $^\circ/\text{sec}$ ).
1.	Shot-Noise	$1.7e^{-7}$	$1.66e^{-6}$

2.	Back Scattering effect	0.54	6.4
3.	Shupe effect	$7.8e^{-6}$	$2.4e^{-5}$
4.	Kerr effect	$6.7e^{-15}$	$2.17e^{-12}$
5.	Faraday effect	$4.47e^{-8}$	$4.5e^{-7}$

Table.1. Comparison of noise sources.

While comparing PM fiber sensor coil with SM fiber as sensor coil, PM fiber gives low shot- noise but main noise sources backscattering noise and Kerr noise are high in value. Thus the above evaluation provides a proper modulation technique to minimize the backscattering and Kerr effect noise with PM fiber as a sensor coil.

## V.CONCLUSION

We have theoretically evaluated the bias of the optical passive resonator gyroscope (OPRG) caused by various deleterious effects in the ring resonator formed by single mode(SM) fiber and compared with polarization maintain (PM) fiber. We observed theoretically low shot noise,  $\delta\Omega_s = 1.66e^{-60}/\text{sec}$  and higher backscattering noise,  $\delta\Omega_B = 6.4 \text{ }^\circ/\text{sec}$  using PM fiber as sensing coil, compared with SM fiber as sensing coil. By modulating CW and CCW beams at different phase in our set up we can minimize drift due to backscattering noise and low shot noise, by using PM fiber as a sensor coil to observe minimum drift at output.

## VI.REFERENCES

[1]. W.K. Burns (ed.), Optical fiber rotation sensing, Academic Press Inc., (1994).

- [2]. R.E. Meyer, Ezekiel, D.W.Stowe, and V.J.Tekippe, "Passive fiber-optic ring resonator for rotation sensing" Opt. Lett. 8(12), 644-646(1983).
- [3]. K.Iwatsuki, K. Hotate, and M. Higashiguchi, "Kerr effect in an optical Passive ring resonator gyro," J. Light wave technol. 4(6), 645-651(1986).
- [4]. K.Hotate, and K. Tabe, "Drift of an Optical fiber gyroscope caused by the Faraday Effect: influence of the earth's magnetic field," Appl.Opt.25 (7), 1086-1092(1986).
- [5]. D.M. Shupe, "Thermally induced no reciprocity in fiber-optic interferometer," Appl.Opt. 19(5), 654-655(1980).
- [6]. K. Iwatsuki, K. Hotate, and M. Higashiguchi, "Effect of Rayleigh backscattering in an optical passive ring-resonator gyro," Appl.Opt.23 (21), 3916-3924(1984).
- [7]. K. Takiguchi, and k. Hotate, "Method to reduce the optical Kerr-effect-induced bias in an optical passive ring-resonator gyro." IEEE Photo. Technol.Lett. 4(2), 203-206(1992).
- [8]. K. Hotate, K. Takiguchi, and A. Hirose, "Adjustment-free method to eliminate the noise induced by the backscattering in an optical passive ring-resonator gyro," IEEE Photo. Technol.Lett.2 (20), 75-77(1990).
- [9]. H. Ma, Z. He, and K.Hotate, "Reduction of backscattering induced noise by carrier suppression in waveguide type optical ring resonator gyro" J.of.Light Wave Technology, 29(1), 328-331(2009).
- [10]. X. Wang, Z. He, and K. Hotate. "Reduction of Polarization-fluctuation induced drift in resonator fiber optic gyro by a resonator with twin  $90^\circ$  polarization-axis Rotated splices," Opt. Express, 18(2), 1677-1683(2010).
- [11]. H. Ma, Z. Jin, C. Ding and Y. Wang, "Influence of spectral Line Width of Laser on resonance characteristics in fiber ring resonator," Chinese Journal of lasers (in Chinese), 30(8), 731-734(2003).